Influence of tensile straining and fibril angle on the stiffness and strength of previously dried kraft pulp fibers

JOHN M. LONG AND WARREN J. BATCHELOR

ABSTRACT: It has long been known that in individual wood fibers, the tensile mechanical properties are heavily determined by the nature of the cellulose chains in the fibers. Both elastic tensile modulus and strength are directly related to the fibril angle, which is the steepness with which the cellulose chains wind their way around the fiber in the secondary wall of the middle layer, named the S_2 layer. Classic work from the 1970s measured modulus and strength in wood fibers as a function of the fibril angle and compared the results with theoretical models. The measurements were hampered by the presence of defects in the fibers, some which occurred naturally and others which resulted from pulp processing. In this study, we performed more accurate measurements of strength and modulus in single fibers of radiata pine by loading the fibers in cycles, gradually pulling some of the defects out of the fibers in an attempt to obtain defect-free values of modulus and strength. We then plotted these properties against measured fibril angle and compared our results with theoretical models. The results show that even when the fiber had reached maximum load before fracture, at a given value of fibril angle, it still had a measured modulus that is around half the theoretically expected value. The results suggest that the load required to fully remove defects from the fibers may be larger than the fibers can bear before fracturing.

Application: Information contained in this investigation will help paper researchers and engineers better understand the relationship between processing defects and mechanical properties of single wood fibers.

In single wood fibers, longitudinal mechanical properties, such as strength, stiffness, and breaking strain, play a large role in determining mechanical properties in the paper manufactured from these fibers. In a wood fiber, the thickest component is the secondary wall of the middle layer, named the S_2 layer [1,2]. Because the S_2 layer is the thickest, the mechanical properties of this layer determine the overall properties of the fiber. The cellulose microfibrils wind their way around the fiber in a helix. The steepness of this helix determines the fibril angle. This angle influences the fiber's properties: density, strength, and tensile elastic modulus, as well as expansion and shrinkage from fiber processing [3-8]. The main factors that control fiber mechanical properties are the fibril angle of the S_2 layer [9,10], any defects in the fiber [11], and the amount of shrinkage of the fiber as it dries [12]. Fibers that are held under restraint as they are dried are stiffer and stronger than those that have been allowed to freely dry. Similar microstructural and mechanical behavior can be found in the fibers of some plants, such as flax [13].

The fibril angle strongly influences the longitudinal mechanical properties, because the bonds along the cellulose chains are much stronger than the bonding between the chains. Despite the importance of fiber mechanical properties to paper properties, there are few sets of data in the literature in which stiffness of single fibers has been measured as a function of fibril angle. The lack of data is probably because such measurements are quite difficult to obtain. In addition to measuring the fibril angle, the fiber cross-sectional area must also be measured in order to convert the measured loads into stresses. Perhaps the most well known of these is the pioneering work by Page, El-Hosseiny, and their colleagues [9,10]. This one full set of measurements was made over 40 years ago, and only fibers from white and black spruce trees were tested. Their data showed that while the elastic modulus and strength of fibers are approximately constant at very low fibril angles (cellulose chains aligned with the fiber longitudinal direction), they fall rapidly for fibril angles beyond 5° or 10°. At fibril angles of 40°, the modulus is reduced to about a fifth [9] compared to fibers with fibril angles between 0 and 10°. More recent investigations on single fibers are consistent with the results presented by Page, but the data sets only contained very small numbers of fibers, such as work on Chinese fir [14] and yew [15]. Other studies have measured mechanical properties of single-fiber southern pine and related the measurements to the position in the trees from which the fibers were collected, noting a relationship between the fibers' strength and stiffness and fibril angle [16-18], but not making an explicit correlation between the two.

Defects can be introduced when the fibers are grown in the wood [19], or more commonly during the pulping process. Defects also become set into chemically pulped fibers when they are dried for the first time. The fibers irreversibly shrink and collapse, a process known as hornification [20-22].

It is known that refining can reverse hornification and can remove defects in previously-dried, chemically-pulped fibers [23]. The forces applied to the fibers in the refiner can straighten fibers and increase the pore volume in the cell wall. Defects in a fiber can cause deterioration of the fiber's mechanical properties. This is especially evident in the work on modulus versus fibril angle in samples of spruce by Page and colleagues, where their data clearly can be seen lying below the theoretical curve for defect-free fibers [9].

Previous work has suggested that it is possible to remove defects in wood fibers by subjecting them to a tensile strain. Experiments on white and radiata pine fibers have shown that repeated cyclic loading in tension can increase their stiffness [24,25]. As an example, **Fig. 1** (taken from Conn and Batchelor [25]) shows how applying cyclic forces to a fiber can change its mechanical properties. The figure shows a single-fiber tensile fatigue test conducted on a radiata pine fiber, conducted in a custom-made tensile test rig designed to eliminate sideways movement and thus ensure uniaxial tension forces. The fiber had been allowed to freely dry before testing. In the test, ten loading cycles of 0–200 mN were performed. Figure 1 shows a very large difference between the initial and subsequent loading cycles. The loading curve for the first cycle has a substantially lower slope than the unloading curve, resulting in substantial plastic strain in the fiber. In the second and subsequent cycles, the loading and unloading curves have similar slopes to the unloading curve of the first cycle, indicating little change in the elastic modulus and no further plastic deformation during these loading cycles. Thus, the initial cyclic load had substantially stretched the fiber (a plastic strain of around 3% for the fiber shown here), possibly removing a defect, such as that of the shrinkage that occurred during the drying process, and thus increasing its stiffness in subsequent cycles. The data shows that at each point on the initial loading curve, the fiber is being stretched. At around 50 mN, there is a sudden increase in extension with little increase in force, 1–1.5 μm. One possible explanation for this effect is that a large defect has been pulled out, such as a kink. Similar load-extension curves to that shown in Fig. 1 have also been observed for white-pine TMP fibers [24]. For a single fiber test of the type shown in Fig. 1, the difference between the modulus in the initial and subsequent cycles is controlled by the degree of restraint under which the fiber is dried, with the largest differences occurring when the fibers are dried unrestrained. Sheets that are restrained as they dry tend to be stiffer and have higher failure loads, because the fibers have not been allowed to shrink as much as unrestrained sheets [26].

In the studies previously cited, where strength and stiffness were related to the fibril angle, all the mechanical tests employed by the respective research groups used single-cycle tensile tests, where the fiber was pulled in tension once, and load and elongation were measured until the fiber fractured. Apart from the study by Wild and colleagues [24], one other study investigated cyclic loading in fibers of ginkgo, juniper, and Norway spruce [27]. The authors presented a model of the fibers' "work hardening" through dynamic chemical effects at the molecular level. The investigation presented in this paper is more on the microscopic rather than on the nanoscale level. Our aim is twofold: using radiata pine rather than spruce fibers, we wish to repeat the work of Page and co-workers by measuring the elastic modulus and strength as a function of fibril angle for different species. It is also the goal of this work to examine how loading these fibers in cycles changes their mechanical properties. We hoped to see whether cyclic loading has reversed the shrinkage and defects produced during drying.

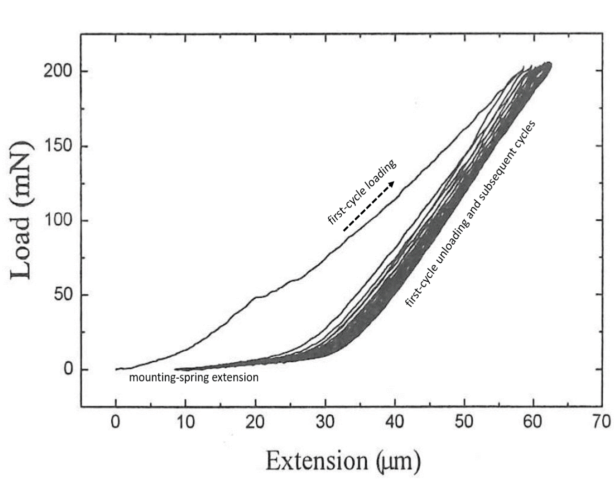

1. Typical dry radiata pine fiber load-extension curves, 10 cycles, taken from Conn and Batchelor [25]. During the first 10–20 μm of extension, the rig's mounting springs stretch slightly before the fiber takes up the load.

EXPERIMENTAL METHOD

The method chosen was to apply a cyclic tensile load to a single fiber, with the maximum load in a cycle increased in each successive cycle. This methodology was chosen because an increase in elastic modulus produced by stretching the fiber in one cycle can only be measured in a subsequent loading cycle. Thus, by gradually increasing the maximum load, the change in modulus can be measured as a function of the maximum load applied. These measured moduli were then compared with the theoretical modulus calculated from the measured fibril angle for the fiber to determine how much of the strength potential of the fiber has been recovered by the tensile loading applied to the fiber.

To give a wide range of fibril angles, two radiata pine wood samples were selected from sections in a core. The bulk fibril angle along a radiata pine core was measured by means of X-ray diffraction [28]. The two wood samples were then pulped in a conventional kraft process by using a solution of sodium sulfide and sodium hydroxide and then cooking at 140°C for 2 h. Prior to pulping, each piece of wood was wrapped in fine wire mesh that held the samples together during pulping. Upon completion of the pulping, six small

2. Confocal images of one typical fiber's cross section, determined by the method of Xu et al. [29]. From three measurements, the average wall thickness was determined to be 3.1 µm ± 10%, an equivalent diameter of 25 µm, and a cross-sectional area of 190 µm².

clumps of pulp were taken from various sections of the samples. To remove most of the hemicellulose from the fibers, each clump was separately bleached in a chlorine dioxide (ClO_2) solution (6.85g ClO_2/L) for 3 h at 70°C. The clumps were then dispersed in water to separate the fibers, and then they were allowed to freely dry on a glass microscope slide. Between 15 and 20 fibers from each clump were randomly selected and mounted between small aluminum tabs using an epoxy cement that was allowed to set over three days. After mounting, the cross-sectional areas of the fibers were determined by means of confocal light microscopy [29]. **Figure 2** shows a sample cross section from one fiber.

The fibril angles of the same fibers were then determined by means of a confocal microscope and an analyzer crossed with polarization of the incident laser light [30]. The fibril angle was determined by the angular position of the microscope stage when the image of fiber rotating on the microscope stage reached optical extinction. A few fibers showed little or no optical extinction. One reason that we considered for this was that perhaps some of the mounting epoxy wicked up the fiber and thus interfered with the optical effects. Such a condition would interfere with the mechanical tests and lead to dubious results. We discounted this possibility firstly because the mounted fibers were directly examined with a microscope to make sure this did not happen. Secondly, in the development of the test method, the action of epoxy as a mounting glue was investigated very carefully and no ill effects were observed [25]. Thirdly, other research groups have also used epoxy for mounting fibers and reported no wicking or other ill effects [14,24,31]. Perhaps, as cautioned by El-Hosseiny and Page [32], there were further, intrinsic anomalies in those fibers that interfered with optical extinction from the cellulose in the S_2 layers. Regardless of the reason, those fibers where optical extinction was difficult to obtain were deleted from the analysis. The comparison between the bulk fibril angles in the wood core measured by X-ray diffraction and those measured by confocal microscopy on individual fibers was published previously [33] and showed excellent agreement. Near the surface of the trunk, less than 20 mm from the bark, the average bulk fibril angle was 6°. The bulk fibril angle increased with distance into the tree to about 30° at a depth of 80 mm. Compression wood had an average fibril angle of 37°.

To ensure that environmental effects would not influence the properties of the fibers, the testing laboratory was held constant at 23°C and 50% relative humidity. The tensile testing of the single fibers was done using an attachment for an Instron universal tester (Instron; Norwood, MA, USA), which was designed to ensure that the load was only applied uniaxially along the fiber. The details of the apparatus and analysis method are described by Conn and Batchelor [25]. Once the test sample was mounted, the gauge length was measured via a travelling microscope. Typical gauge lengths were between 0.4 and 1.0 mm. Using a 1 N load cell, each fiber was tested under cyclic loading conditions with the maximum load in the first cycle set to 0.02 N. Thereafter, the maximum load was incremented for each successive cycle by 0.02 N until the fiber failed. The raw data for each tensile test were a succession of load-extension curves. For each cycle in a test, the slope of the load-extension curve as a function of extension was calculated by means of numerical differentiation. The slope-extension data for each cycle was then corrected for the test rig's mounting spring by subtracting the internal spring constant, which gives each plot of slope versus extension a small vertical offset. Then, the maximum slopes for loading and unloading were determined from the corrected data. The maximum slopes were combined with the measured gauge length and cross-sectional area to calculate the elastic modulus for the fiber in the loading case and for the unloading case. Finally, the breaking load was noted and the breaking stress was calculated. For each successfully tested fiber, the elastic modulus in the first cycle, the elastic modulus in the final complete cycle, the breaking load of the fiber, and the degree of plastic deformation at the commencement of the final cycle were extracted from the test data.

As an example of our technique, **Fig. 3** shows the raw load-extension data for the third cycle of a fiber with a fibril angle of 24° after tensile testing. This sample was taken from a piece of compression wood, and it was expected to have a relatively high fibril angle. Beforehand, this fiber had a mea-

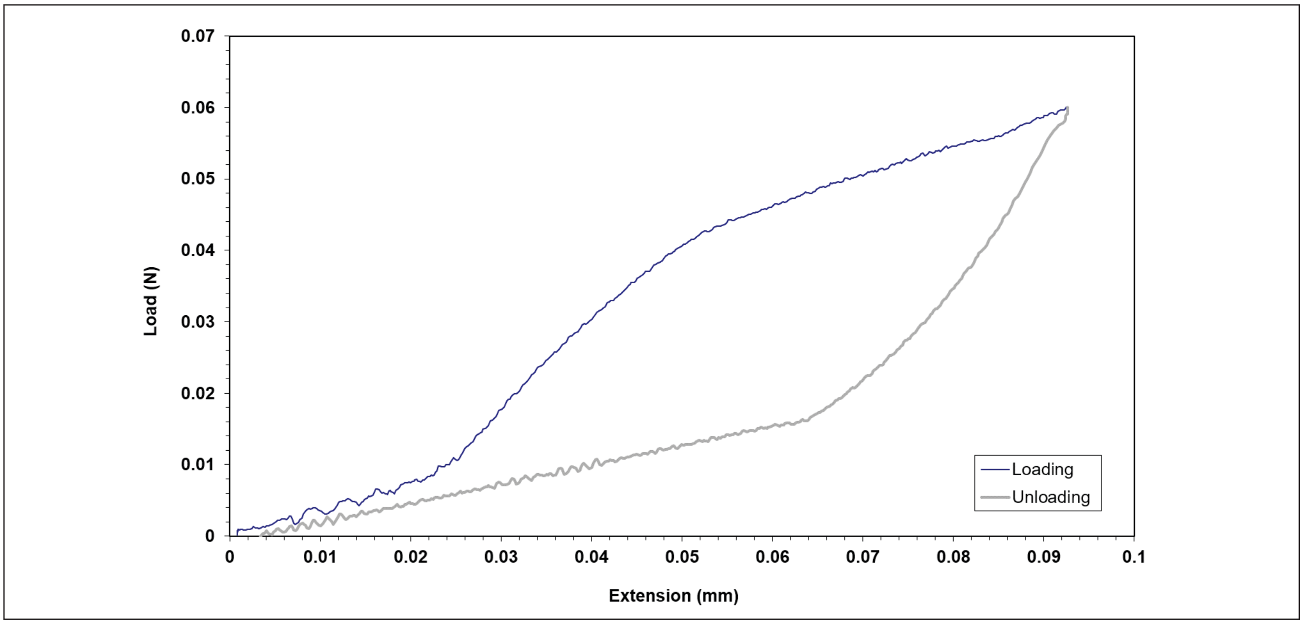

3. Load-extension curve of the third cycle of a single radiata pine fiber.

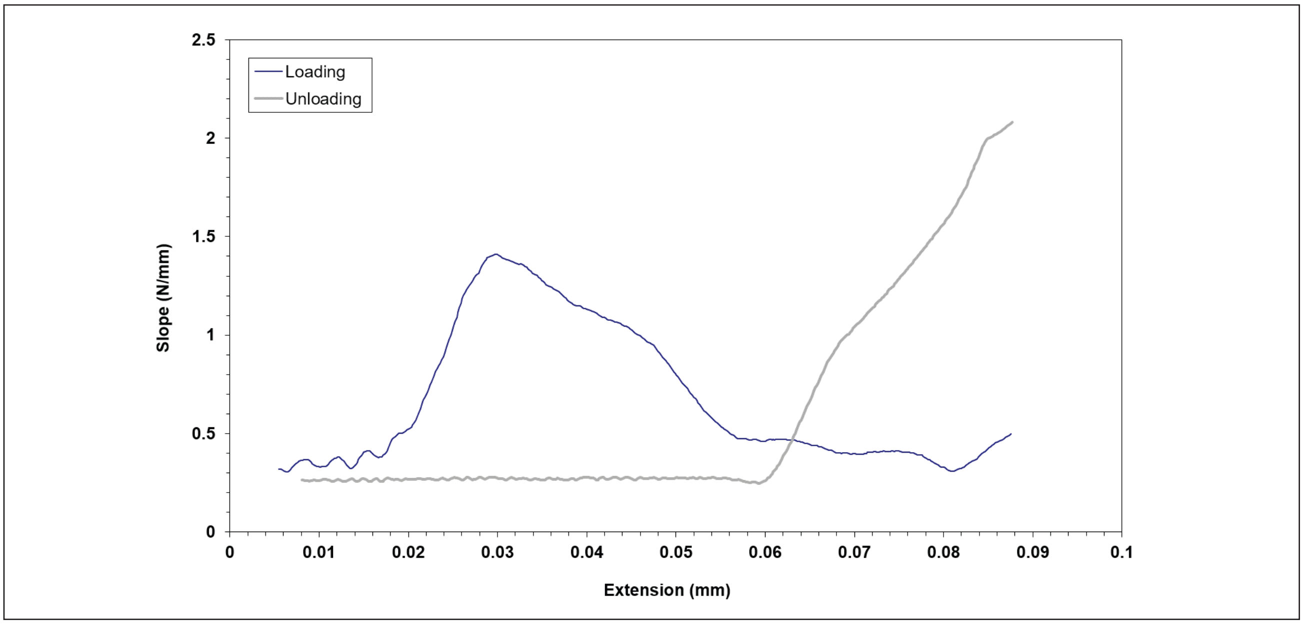

4. Slope of the load-extension curve of Fig. 3's fiber. The presence of the mounting spring is visible in the vertical offset of 0.3 N/mm.

sured fibril angle of 43°. At first, the load was absorbed by the mounting spring in the test apparatus. The mounting spring, shown in Fig. 1 of reference [25], ensure that there is no lateral movement in the loading of the fiber. At an extension of about 0.025 mm, the fiber begins to bear the load. In this cycle, the load was increased to 0.06 N, and then decreased back to zero. The fiber shows yielding at an extension of 0.045 mm. Plastic deformation is evident from the large hysteresis in the curves. The slope of the load-extension curve is related to the stiffness of the fiber (**Fig. 4**). On loading, the fiber shows the maximum slope at an extension of around 0.03 mm. However, the slope is larger still at the beginning of the unloading part of the test. The effect of the test rig's mounting spring was subtracted out from the slope data by averaging the slope data at the start of the test before the slope begins to rise (about 0.3 N/mm in this case) and subtracting this vertical offset from the data set. Of the 80 fibers that were initially mounted, 21 were successfully strained to fracture, and the fibril angle on these fibers was remeasured after completion of the cyclic tensile tests.

According to our theory, and as suggested by Page and colleagues [9], before mechanical testing, a given fiber contains kinks, knots, pores, and other defects. Placing the fiber gradually under tension pulls the defects associated with fiber

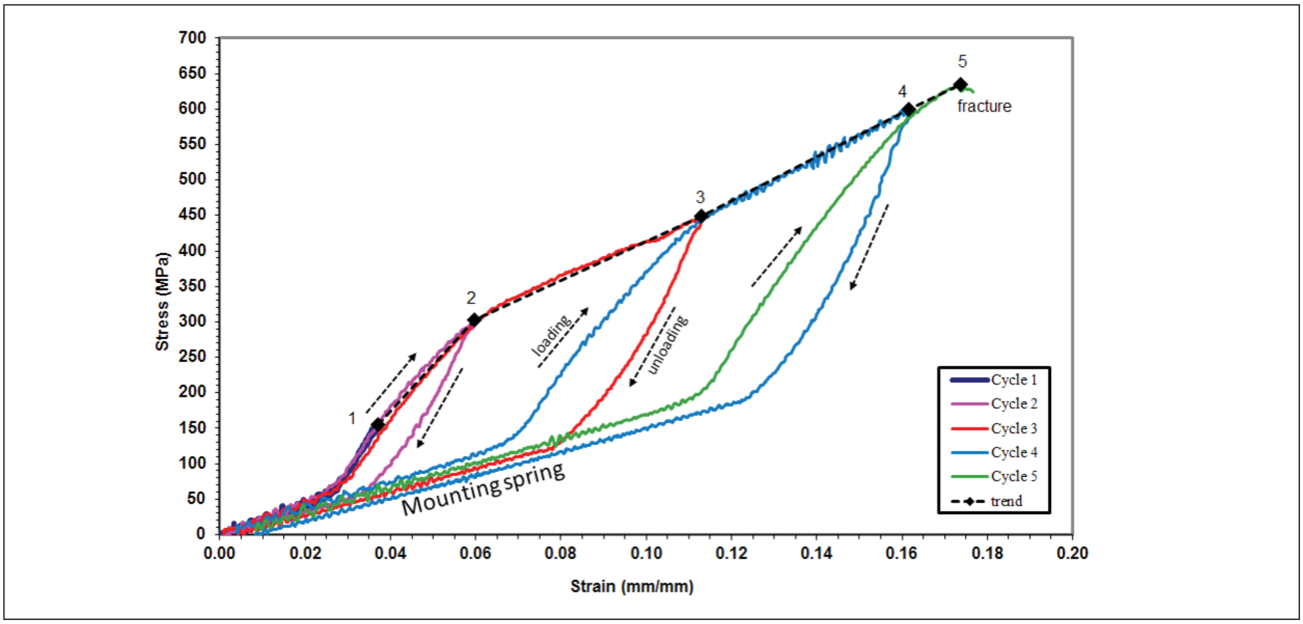

5. Stress-strain curve of a single radiata pine fiber in cyclic loading. The maximum load has been increased in 0.02 N increments, until the fifth cycle, where the sample has fractured. The fibril angle decreased from 43 ±2° before cyclic loading to 24 ±1° after loading. The numbers indicate cycle number, the squares indicate the overall trend, and the arrows indicate loading or unloading.

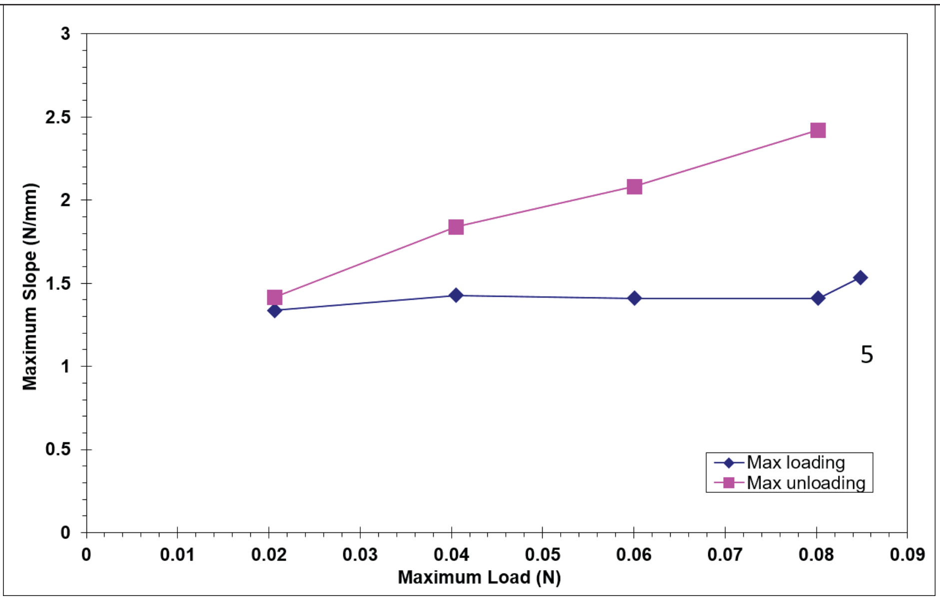

6. Slope of the load-extension curves for Fig. 5's fiber. A greater stiffness is shown in the unloading cycles, which suggests that with plastic deformation, the fiber modulus is increasing.

processing out of the fiber. As the defects are removed, we expect to see the fiber becoming stiffer (increased modulus) from cycle to cycle. Also, we expect the fibril angle to decrease as the number of cycles increase because the tensile loads tend to pull the cellulose chains more parallel with the length of the fiber. Thus, to determine the properties of "defect-free" fibers, we used fibril-angle measurements after cyclic loading was complete. We also compared modulus (slope of a stress-strain curve) in both loading and unloading cases.

RESULTS

Figure 5 shows an example of the results obtained from the representative fiber of Figs. 3 and 4. Prior to mechanical testing, the fibril angle of this fiber was measured to be 43 ±2°. The gauge length of this particular fiber was 0.82 mm, and its measured cross-sectional area was 134 μm². The second loading cycle shows similar behavior to that seen in the first loading cycle of Fig. 1. The slopes of the loading curves are lower than the corresponding slopes of the unloading curves

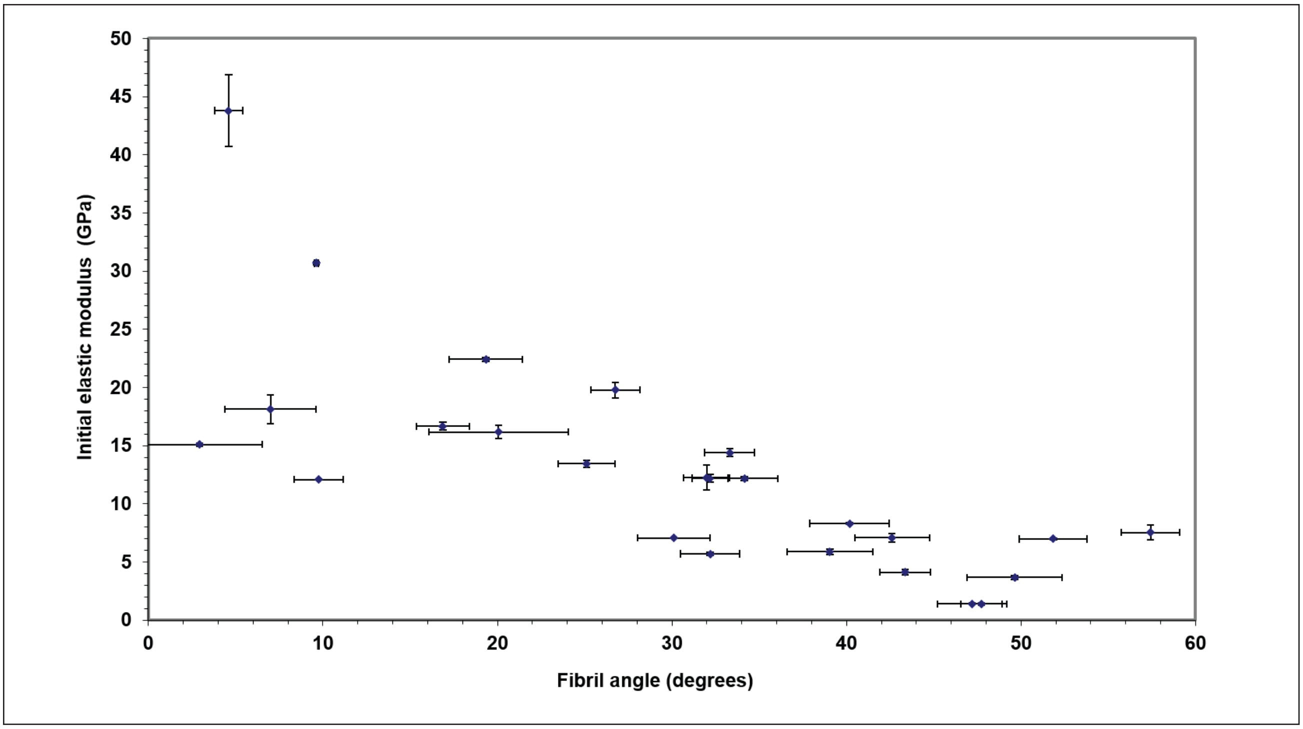

7. Initial elastic modulus determined from the slope of the stress-strain curve in the initial loading cycle, as a function of the fibril angle measured before the commencement of mechanical testing.

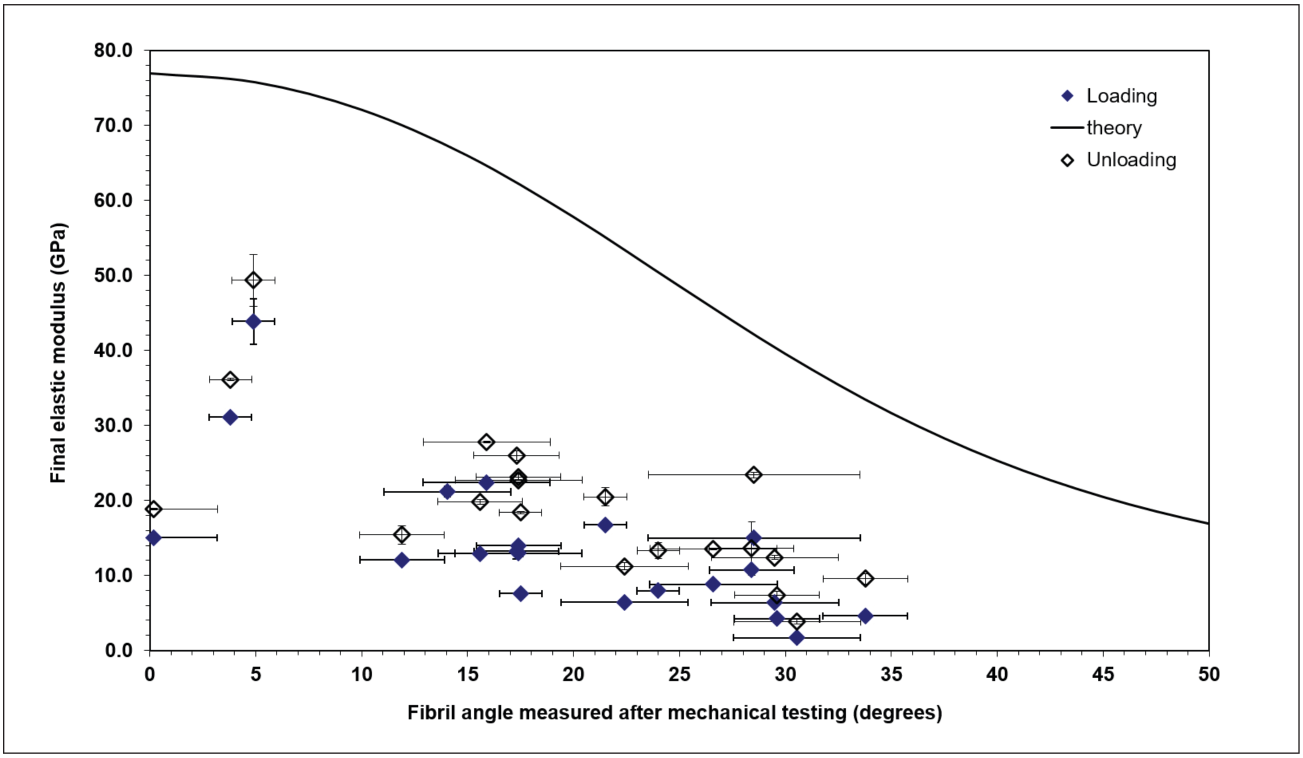

8. Elastic modulus measured in the final cycles before fracture as a function of the fibril angle measured after fracture. Closed symbol is for loading in the final cycle, and open symbol is for final unloading. The solid line is the maximum attainable modulus, calculated from the theoretical work of Page et al. [9, p. 116].

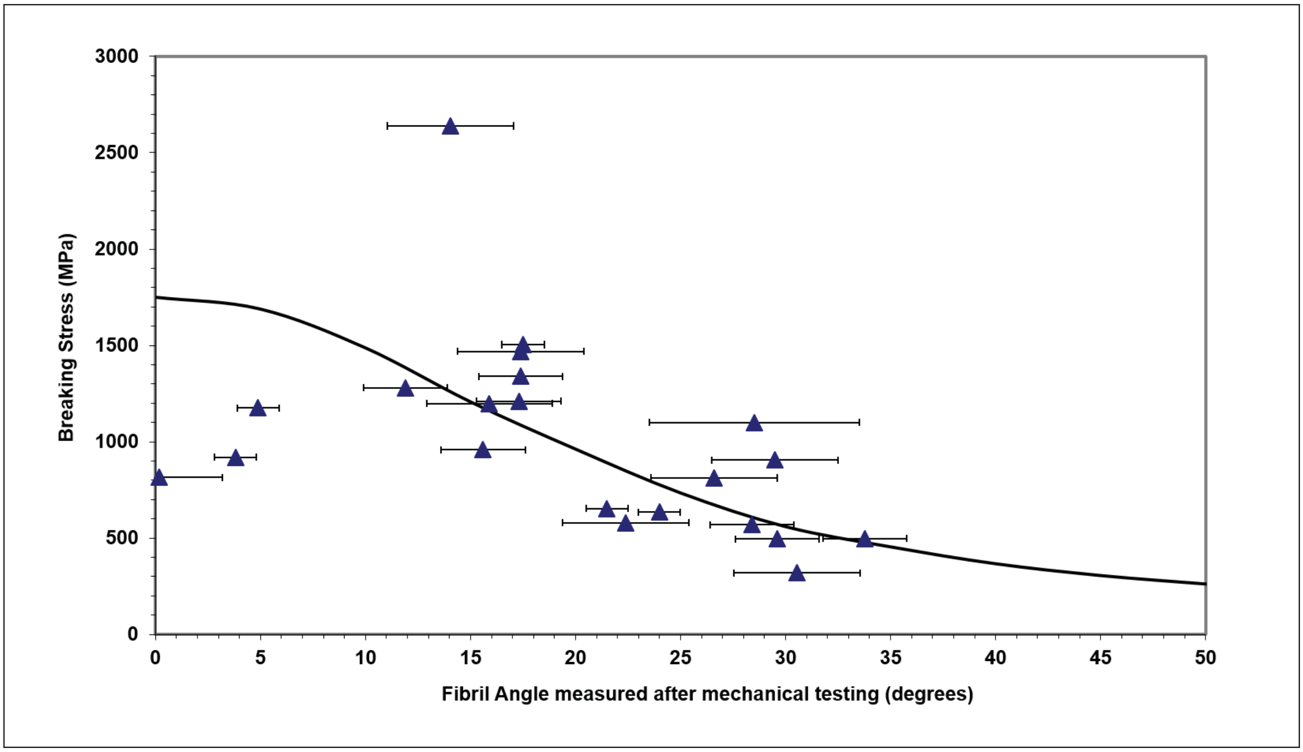

9. Breaking stress achieved in the final cycle before fracture versus fibril angle. The curve represents the theoretical limit for spruce as calculated by El-Hosseiny and Page [34].

(**Fig. 6**), as expected, and the sample has undergone substantial plastic deformation during loading. In many cases, we observed that the loading curve of the next cycle shows a similar modulus to the unloading while the sample is being loaded to the maximum load attained in the previous cycle. The sample then begins to plastically deform again once the maximum load from the previous cycle is exceeded. The process was repeated until the sample fractured. This fiber completed four cycles and broke in the fifth. The slope of the load-extension data was a maximum in the fifth cycle for loading and in the fourth for unloading. The data show that the stiffness of the fiber increases with the amount of plastic deformation, with the biggest change occurring between the first and second cycles. From the maximum slope values, the elastic modulus for this fiber was determined to be 8.0 ±0.4 GPa while loading the fiber, and 13 ±1 GPa while unloading. One can call the elastic modulus determined in the loading case the initial modulus and that in the unloading case the final modulus. Strength of a fiber was determined by the maximum stress on the fiber prior to fracture. In the case of the sample fiber discussed here, the strength was 634 MPa. After mechanical testing, the fibril angle was remeasured and found to have decreased to 24 ±1°. Some of the fibers tested broke after only three cycles. Many fibers passed 10 cycles, and one fiber completed 20 cycles before fracture. We observed the general behavior of stiffening with successive cycles repeatedly in all the fibers that we tested.

Elastic modulus results

We observed that for most, but not all, fibers, the measured fibril angle before tensile testing was greater than that after tensile testing, ranging from near 0 to 58°. **Figure 7** shows the initial elastic modulus obtained in the initial loading cycle for all fibers. We use caution in calling these values "moduli" because as the previous discussion has indicated, the initial loading data had no measurable elastic region, and plastic deformation occurs continuously throughout the loading cycle. In further analysis here, we use the fibril-angle data measured after tensile testing. Replotting these results as a function of fibril angle measured after tensile testing yields **Fig. 8**. Also plotted on this graph is the theoretical curve for radiata pine as calculated from Page's analysis [9]. The unloading values are significantly higher than the loading values, especially at higher fibril angles. This confirms the hypothesis that the fibers become stiffer as cyclic loading proceeds and reach a maximum with the final unloading cycle.

Strength results

Figure 9 shows our results for breaking stress versus fibril angle. El-Hosseiny and Page [34] calculated a theoretical limit for similar data in spruce fibers, and this curve is included in the plot. Between 10° and 35°, the curve fits the data rather well. However, strengths for fibril angles lower than 10° are much lower than what one might expect from the theory. Further experiments may shed more light on this surprising result.

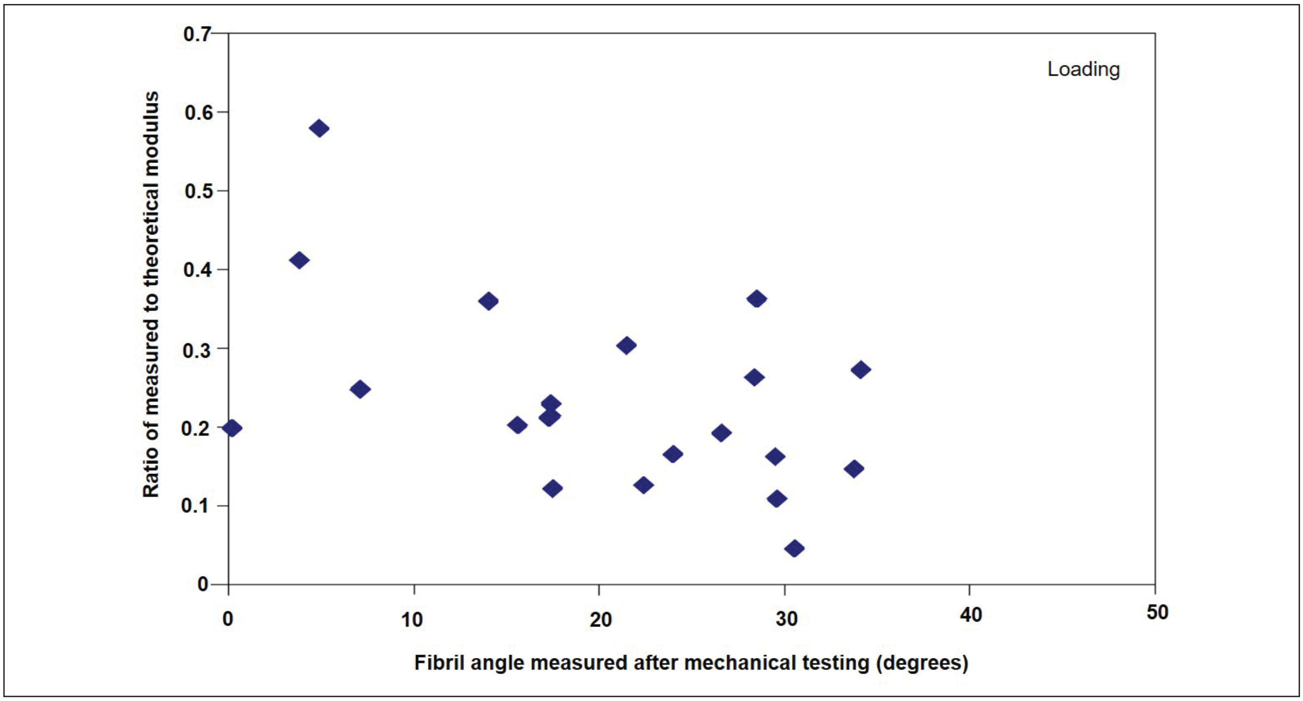

10. Ratio of modulus measured in the last loading cycle to the theoretical modulus.

DISCUSSION

We observed significant plastic deformation in many of the fibers, and that of Fig. 5 is typical. After bleaching, these fibers were allowed to dry without restraint and we suggest that the plastic deformation is due to several sources. First, some of the shrinkage and defects, which had been introduced into the fiber as it was dried, have been pulled out. Second, the fibril angle of the fiber tends to decrease as the fiber is loaded. The reduction in the pitch at which the fibrils are helically wound will reduce the cross-sectional dimensions of the fiber and increase the length. It is interesting that for the fiber of Fig. 5, the plastic deformation seems to increase continuously with increasing load. While an approximate yield point is visible in cycles 3 and 4, this apparent yield stress increases with each cycle.

Figure 8 shows the elastic-modulus results. In this figure, the elastic modulus in the final loading cycle is plotted against the fibril angle after testing—that is, after the fiber has fractured. In comparison to the results in Fig. 7, several interesting trends can be seen. The first trend is that the mechanical loading has, in general, reduced the fibril angle, with the average fibril angle falling from 29° to 19°. Furthermore, the largest reductions in fibril angle occur for fibers that had the highest initial fibril angle. These figures further show the large increase in elastic modulus of the final cycle before fracture compared to the slope of the stress-strain curve in the initial cycle. However, despite the increase in modulus as the sample is stretched out, it can be seen that the measured modulus before failure is still much less than the theoretical value. The ratio of the measured to the theoretical modulus was plotted in **Fig. 10**. The data shows a general upward trend with decreasing fibril angle, with the fibers with lowest fibril angles tending to attain the highest percentage of the theoretical maximum. The average ratio over the whole set of data is only 22%. The results show that even when the fibers have reached the maximum load before fracture, they still have values of elastic modulus that are around half that predicted by theory, given the fibril angle of the fiber. From this result, we conclude that the load required to fully remove all defects from the fibers may be larger than what the fibers can bear before breaking. There are certainly some defects that would not be removed by cyclic straining, such as pits in a side wall. What interests us here are those defects that result from processing and shrinkage as the fibers dry.

The information that comes from performing the experiments this way is much more than could be obtained with conventional single-cycle testing. The mechanical properties of the fibers after drying can be measured and compared with the modulus obtained after the fiber has been stretched again. The cyclic loading method allows for these changes to be monitored at different levels of stress, given that the sample is periodically unloaded. Deformation of wood fibers during cyclic loading warrants further study. For instance, these experiments could be performed on another species of wood. Furthermore, the fibers could also be subjected to detailed microscopic analysis to observe processing defects directly before and after cyclic loading. Finally, the stiffening of the fibers during cyclic loading may be a combination of both reducing defects through cyclic strain and any resulting reduction of the fibril angle. Theoretical modelling of the mechanical behavior of loaded fibers with defects and a simultaneous change in the fibril angle may shed some light on this.

CONCLUSIONS

The tensile mechanical properties of single fibers of radiata pine were studied as a function of fibril angle (the steepness with which cellulose molecules wind their way around the S_2 layer of the fiber). In an attempt to determine the elastic modulus and strength of defect-free fibers, single fibers were loaded in cycles of increasing load, noting the slope of the stress-strain curve while loading and unloading in each cycle. The fibers had varying values of fibril angle ranging from near 0 to 35°. For each fiber, the maximum slope of the stress-strain curves was taken to be the elastic modulus. Strength was taken as the breaking stress. The measured elastic moduli of the fibers were observed to increase from that measured in the first cycle to that measured in the final cycle, confirming the hypothesis that fibers can be stiffened by means of cyclic straining. At the same time, the measured values of fibril angle tended to decrease from before mechanical testing to after mechanical testing, especially in the case of fibers with higher initial fibril angles. Plots of elastic modulus versus fibril angle and strength versus fibril angle were similar in shape to previously published plots taken from data obtained from spruce fibers. Our measured values of modulus were well below classic theoretical predictions, while our measurements of strength showed slightly better agreement with the classic theoretical model. We conclude from these results that due to strength limitations, cyclic loading was insufficient to remove all the defects from the fibers and thus obtain the "true" value of elastic modulus. Nonetheless, the results are quite interesting and worthy of further study with different species of wood. **TJ**

ACKNOWLEDGEMENTS

The financial support of the Commonwealth Government of Australia through the Australian Research Council is gratefully acknowledged. JML acknowledges support from a Deakin-University research fellowship while this work was being performed. We also thank A.B. Conn and Y. Filonenko for their valuable assistance during this project.

LITERATURE CITED

1. Barnett, J.R. and Bonham, V.A., *Biol. Rev.* 79(2): 461(2004).
2. Mark, R. and Gillas, P., in *Handbook of Physical and Mechanical Testing of Paper and Paperboard* (R. Mark, Ed.), Marcel Dekker, New York, 1983, vol. 1, chap. 10.
3. Donaldson, L., *IAWA J.* 29(4): 345(2008).
4. Courchene, C.E., Peter, G.F., and Litvay, J., *Wood Fiber Sci.* 38(1): 112(2006).
5. Farber, J., Lichtenegger, H.C., Reiterer, A., et al., *J. Mater. Sci.* 36(21): 5087(2001).
6. Fang, S.Z., Yang, W.Z., and Fu, X.X., *J. For. Res.* 15(4): 261(2004).
7. Reiterer, A., Lichtenegger, H., Tschegg, S., et al., *Philos. Mag. A* 79(9): 2173(1999).
8. Burgert, I., Frühmann, K., Keckes, J., et al., *Trees* 18(4): 480(2004).
9. Page, D.H., El-Hosseiny, F., Winkler, K., et al., *Tappi* 60(4): 114(1977).
10. Page, D.H., El-Hosseiny, F., Winkler, K., et al., *Pulp Pap. Mag. Can.* 73(8): 72(1972).
11. Mohlin, U.B., Dahlbom, J., and Hornatowska, J., *TAPPI J.* 79(6): 105(1996).
12. Jentzen, C.A., *Tappi* 47(7): 412(1964).

ABOUT THE AUTHORS

An opportunity for a collaborative research project arose between Deakin and Monash Universities, and this research enhances the field of paper research in that it attempts to extend previous work on mechanical properties of wood fibers in an enhanced way that has not been tried before.

The preparation of individual fibers for tensile testing was the most difficult aspect of this work. The second most difficult aspect was the lengthy data analysis that was required. Personally, I (Long) discovered new ways of testing single fibers, both mechanically and microstructurally, and I expanded my personal expertise in the general field of materials analysis. I also clearly observed the correlation between fibril angle in wood fibers and their tensile properties.

The most interesting aspect of this work was repeating classic research on fibers, confirming the original results on another species of wood, and then extending the investigation. Surprisingly, even straining the fibers in cycles did not result in the fibers having measurable stiffnesses and strengths matching the theoretical predictions.

Through this research, mills may gain further insight into fiber properties of softwoods and their relationship to the fibril angle. The next step is to repeat the theoretical strength and stiffness calculations for radiata pine fibers by means of modern finite element modeling.

Long

Batchelor

Long is senior lecturer in the School of Engineering, Deakin University, Geelong, Victoria, Australia. Batchelor is associate professor in the Department of Chemical Engineering, Monash University, Clayton, Victoria, Australia. Email Long at john.long@deakin.edu.au.

13. Bourmaud, A., Morvan, C., Bouali, A., et al., *Ind. Crops Prod.* 44: 343(2013).
14. Wang, G., Yu, Y., Shi, S.Q., et al., *Wood Fiber Sci.* 43(3): 251(2011).
15. Keunecke, D., Eder, M., Burgert, I., et al., *J. Wood Sci.* 54: 420(2008).
16. Groom, L., Mott, L., and Shaler, S., *Wood Fiber Sci.* 34(1): 14(2002).
17. Mott, L., Groom, L., and Shaler, S., *Wood Fiber Sci.* 34(2): 221(2002).
18. Groom, L., Shaler, S., and Mott, L., *Wood Fiber Sci.* 34(2): 238(2002).
19. Eder, M., Jungnikl, K., and Bugert, I., *Trees* 23(1): 79(2009).
20. Laivins, G.V. and Scallan, A.M., "The mechanism of hornification of wood pulps," *Transactions of the Tenth Fundamental Research Symposium*, PIRA International, Leatherhead, UK, 1993.
21. Fernandes-Diniz, J.M.B., Gil, M.H., and Castro, J.A.A.M., *Wood Sci. Technol.* 37(6): 489(2004).
22. Page, D.H., *Sven. Papperstidn.* 88(5): R30(1985).
23. Page, D.H., in *Fundamentals of Papermaking Transactions of the Ninth Fundamental Research Symposium* (C.F. Baker and V.W. Punton, Eds.), Mechanical Engineering Publications, London, 1989, Vol. 1, pp. 1-38.
24. Wild, P.M., Provan, J.W., Guin, R., et al., *TAPPI J.* 82(4): 209(1999).
25. Conn, A.B. and Batchelor, W.J., *Appita J.* 52(4): 290(1999).
26. Kiiskinen, H., Paltakari, J., and Pakarinen, P., "Drying and paper quality," in *Papermaking Part 2: Drying* (M. Karlsson, Ed.), Fapet Oy, Helsinki, 2000.
27. Keckes, J., Burgert, I., Frühmann, K., et al., *Nat. Mater.* 2: 810(2003).
28. Evans, R., Stuart, S.A., and Van der Touw, J., *Appita J.* 49(6): 411(1996).
29. Xu, L., Filonenko, Y., Li, M., et al., *Appita J.* 50(6): 501(1997).
30. Batchelor, W.J., Conn, A.B., and Parker, I.H., *Appita J.* 50(5): 377(1997).
31. Mott, L., Shaler, S.M., and Groom, L.H., *Wood Fiber Sci.* 28(4): 429(1996).
32. El-Hosseiny, F. and Page D.H., *Wood Fiber* 5(3): 208(1973).
33. Long, J.M., Conn, A.B., Batchelor, W.J., et al., *Appita J.* 53(3): 206(2000).
34. El-Hosseiny, F. and Page, D.H., *Fibre Sci. Technol.* 8(1): 21(1975).